# Evaluating the potential of topsoil magnetic pollution mapping across different land use classes

Ynse Declercq[a,b,*], Roeland Samson[b], Ana Castanheiro[b], Simo Spassov[c], Filip M. G. Tack[d], Ellen Van De Vijver[a], Philippe De Smedt[a]

[a] *Research Group Soil Spatial Inventory Techniques, Department of Environment, Ghent University, Coupure Links 653, 9000 Ghent, Belgium, Ervdevij.VanDeVijver@UGent.be (Ellen Van De Vijver), Philippe.DeSmedt@UGent.be (Philippe De Smedt)*

[b] *Laboratory of Environmental and Urban Ecology, Department of Bioscience Engineering, University of Antwerp, Groenenborgerlaan 171, 2020 Antwerp, Belgium, roeland.samson@uantwerpen.be (Roeland Samson), ana.castanheiro@uantwerpen.be (Ana Castanheiro)*

[c] *Laboratory for Environmental Magnetism, Geophysical Centre of the Royal Meteorological Institute, Rue du Centre de Physique 1, 5670 Dourbes, Belgium, simo@meteo.be*

[d] *Laboratory of Analytical Chemistry and Applied Ecochemistry, Department of Green Chemistry and Technology, Ghent University, Coupure Links 653, 9000 Ghent, Belgium, Filip.Tack@UGent.be*

* Corresponding author: Fax: +3292646247
Tel: +3292646042

E-mail: Ynse.Declercq@UGent.be

## Abstract

Soil magnetic measurements are used increasingly to estimate the impact of airborne, combustion-related particulate matter (PM) pollution in dense measurement grids. Although many studies have proven the potential of topsoil magnetic measurements in environmental monitoring, their application is not straightforward when factors such as parent material or land use have to be accounted for. Often, the influence of land use on the soil magnetic signal is circumvented by targeting forest soils, where deposited magnetic particles are best preserved in the topsoil. However, when large forests are absent, e.g. in densely populated areas or environments with more heterogeneous land use, this approach often impedes reliable and comprehensive spatial sampling. We evaluated if topsoil magnetic pollution mapping across different land use classes, against a homogeneous geological environment of sandy soils, could help increase the spatial reliability of results in regional scale surveys. Although detailed magnetic property analysis and evaluation of trace metal concentrations in soils on arable land, forest and pasture showed the impact of atmospheric pollution, topsoil susceptibility measurements did not allow delineating the magnetic footprint of PM pollution. Land use strongly influenced the distribution of magnetic particles through soil, and the evaluation of anomalous magnetic topsoil enhancement required the integration of downhole susceptibility soundings. We conclude that topsoil susceptibility mapping remains a useful tool to evaluate PM pollution impact, yet its application potential across land use classes is limited.


Keywords**:** magnetic susceptibility, air pollution, trace metals, spatial analysis, soil

## 1. Introduction

Magnetic measurements are a commonly used proxy for tracing combustion-related environmental pollution, as these processes lead to the emission of magnetic iron oxides.[1, 2] Hereby, trace metals are adsorbed on or incorporated into emitted magnetic particles,[3-5] which are then blown away by wind and

deposited on soil, plant leaves or other receptors where further binding processes might take place. The resulting degree of the receptor's magnetic signature can be used as a proxy parameter for combustion-derived PM deposition and metal pollution.[1] As magnetic measurements are fast and inexpensive, sampling density can be increased compared to conventional gravimetric PM measurements.[6-8] Successful examples include monitoring of tree[2, 9-11] or plant leaves,[12, 13] mosses and lichens,[14-16] and street dust.[17] Yet, soil is the most straightforward and hence most commonly used receptor for magnetically enhanced PM, and soil magnetic measurements are known to be easy, fast and cheap.[18, 19] They are particularly effective in urban and industrial zones marked by household, traffic and industrial combustion,[20-23] where clear correlations are often found between the observed magnetic response and the degree of trace metal pollution in the soil.

Magnetic soil surface measurements enable delineating the magnetic footprint of active pollution sources based on the subsurface record.[11, 24-26] However, as a receptor, soils render a complex magnetic response due to a combined influence of natural and anthropogenic factors,[27-29] often burdening straightforward interpretation of topsoil magnetic data over larger areas. The presence of lithogenic particles derived from magnetic parent material, for instance, impedes the analysis of the anthropogenic magnetic fraction in soil.[30-32] In addition, land use influences the distribution of deposited magnetic particles in the topsoil. In undisturbed forest soils, magnetic particles are adhered to the geochemically active organic-mineral matter in the organic O and humic, mineral Ah horizons, which act as a filter for magnetic PM.[24, 31, 33-40] In the overlying litter layer, particles are only physically attached to the surface of undecomposed organic matter, from where they are easily washed out and transported downwards.[41] As such, the magnetic depth profile shows a distinctive peak in the organic horizons whose thickness determines the depth and kurtosis of the peak.[35, 42] In agricultural soils, magnetic particles are mixed in the plough layer. Here, magnetic depth profiles show a slightly enhanced, homogenized and stable magnetic signal in the upper 30 cm, which complicates evaluating the pollution extent.[11, 36, 38, 40, 43-46] As

topsoil magnetic sensors generally enable investigating the uppermost 8 cm beneath the instrument,[47] surface measurements might not reflect the soil's magnetic depth signature and concomitant pollution status reliably.[19, 48] Land use also affects the lateral, small-scale variability of the topsoil magnetic signature. Whereas surface records in arable lands are rather constant due to ploughing, records in forests show higher variability due to variations in canopy cover, complex PM deposition processes and soil micromorphology.[24, 36, 43] Depending on this local surface magnetic variability, which appears to be positively correlated with the magnetic susceptibility (k),[49] multiple surface measurements are mostly averaged to obtain one representative value. Furthermore, higher and less variable values are usually obtained underneath vegetation or litter, which generally dilute the magnetic surface signal.[49-51] Therefore, these layers should be removed before measuring.[34, 50, 52-54] However, when deployed over larger areas, the aforementioned sampling recommendations do not address differences in soil magnetic susceptibility caused by land use. This introduces uncertainties in susceptibility maps, and hampers correct and uniform assessment of the pollution status of surveyed areas.

Most studies have been limited to forest soils where the canopy easily captures dry deposition and where deposited magnetic particles are subsequently retained in the organic soil layers.[38, 55, 56] It is commonly advised to avoid measurements on arable land,[36] however, in areas with more heterogeneous land use and limited forest coverage, recording such soils is often the only means to allow sampling in a denser grid.[44] Forests only cover 35% of Europe's territory with Estonia, Finland, Sweden, Montenegro and Slovenia having the largest shares.[57] They become even scarcer in more densely populated areas, such as the north of Belgium (Flanders) where they are limited to about 12%.[58] While potentially hampering the interpretation of survey results,[36, 43] combining different land use classes is inevitable when the atmospheric pollution impact in heterogeneous areas on a regional scale is to be investigated. Here, we evaluate the applicability of magnetic pollution mapping in heterogeneous areas by investigating the three dimensional dispersal of magnetic pollutants under the influence of different

types of land use. Alongside detailed assessment of the response obtained for anthropogenic pollutants on three test sites, the potential of large area susceptibility mapping in different land use classes is investigated over a wide study area of approximately 3 km².

# 2. Materials and methods

## 2.1 Study area

The study area is located downwind of a metallurgical factory in the Ghent harbor area, Belgium (Figure 1A).[59] Since 1962, the factory produces goods for different applications mainly in the automotive industry and construction sector, but also for wind turbines, can packaging, household appliances and guardrails.[60] Production starts with the transformation of coal and iron ore into sinter and coke, which are subsequently melted to produce liquid pig iron. The above end products are created via post-treatment of the latter. Considerable investments have been made since the 1990s to decrease emissions of PM via chimneys and diffuse sources (Figure 2).[61]

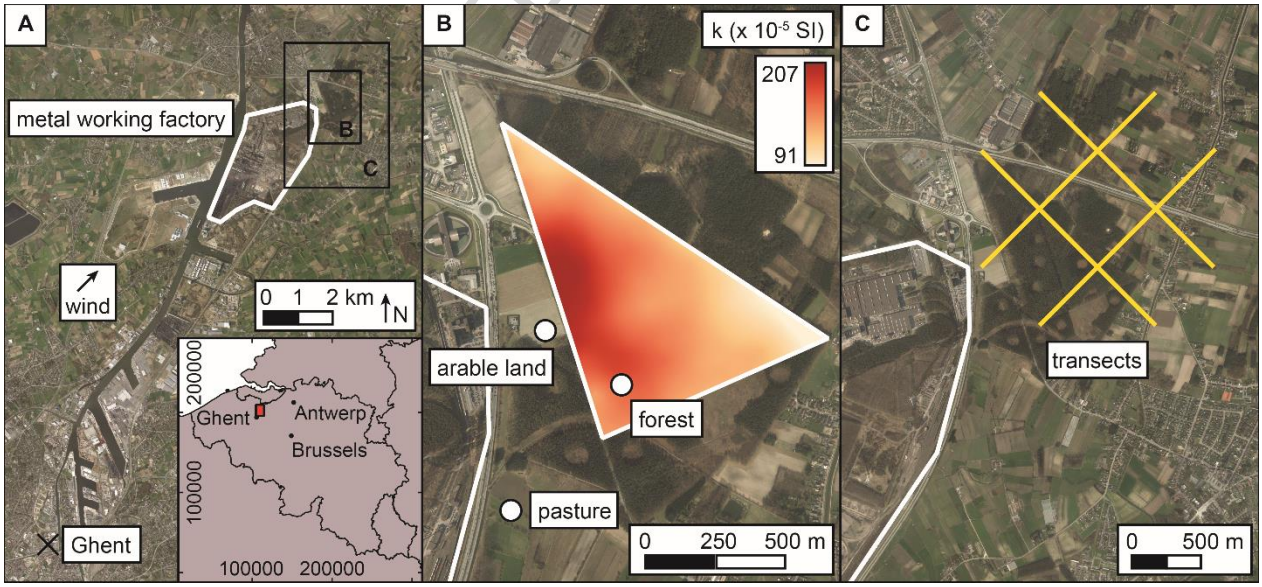


**Figure 1: The study area is located in the north of Belgium, downwind of a metallurgical factory (white line) in the Ghent harbor area (A). In the first step, three 1 m² reference sites (white dots) were selected in arable land, pine forest and pasture (B). The magnetic susceptibility (k) map from previous research[62] is also shown in B. In the second step, four transects (yellow lines) were spread over a larger study area further eastwards of the factory (C).**

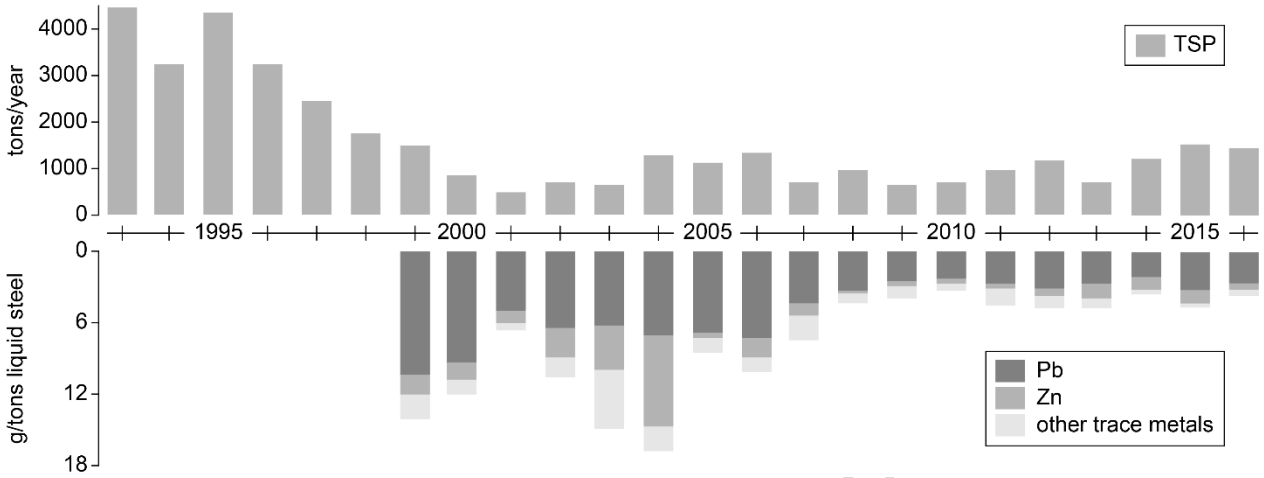


**Figure 2: Yearly total suspended matter (TSP) (1993 – 2016) and trace metal (1999 – 2016) emissions from both diffuse sources and chimney exhaust in the metallurgical factory.[60, 63]**

The plant emitted 178 kg Ni, 326 kg Cr, 432 kg Cd, 890 kg Mn, 997 kg Cu, 2,700 kg Zn, 14,600 kg Pb and 1,200,395 kg $PM_{10}$ in 2016.[64] These values are in accordance with other metallurgical factories, generally known to emit large amounts of Fe, Pb, Zn, Mn and Cu.[23, 39, 65, 66] Furthermore, 93% of the industrial $PM_{10}$ emissions in 2013 in the harbor arose from this factory.[60] Previous studies have indicated considerable magnetic enhancement following industrial activity in the area.[62, 67] Main activities in the harbor include steel and automotive industry, alongside transshipment of iron ores, building materials, grain, and animal or vegetable oils.[68] Monitoring stations in the area registered average values of 24 and 15 µg $m^{-3}$ $day^{-1}$ for $PM_{10}$ and $PM_{2.5}$, respectively, in 2016, i.e. below European PM limits.[69] This also holds for trace metals in $PM_{10}$: averages of 15, 0.4, 1, 3, 11, 13 and 37 ng $m^{-3}$ were measured for, respectively, Pb, As, Ni, Cr, Cu, Mn and Zn between May 2016 and April 2017.[70]

The study area is located on sandy substrate that, in contrast to igneous bedrocks, contains negligible amounts of magnetic minerals,[38, 71, 72] and as such offers a stable diamagnetic background in which any anthropogenic magnetic enhancement will strongly dominate the total observed magnetic response. A reference soil profile (down to 7 m) located 10 km east of the metallurgical factory showed susceptibility values only up to ~20 x $10^{-5}$ SI in the organic soil horizons, below which susceptibility almost dropped to zero (Figure 3).[73] Consequently, the influence of natural magnetic background variations, which can

impede relating the susceptibility signal to anthropogenic contributions in more complex environments,[38, 74] can be considered negligible. Furthermore, the potential of the sandy soils to retain magnetic minerals is limited. Thus, any influences of land use on the presence of magnetic minerals in the topsoil is likely to be clearly reflected.

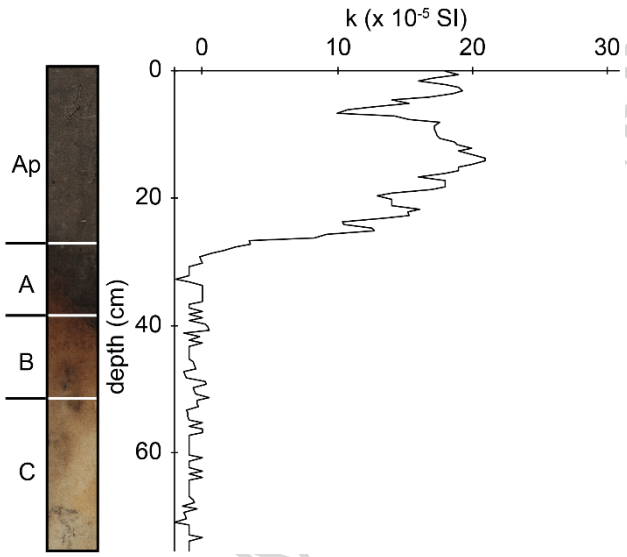


**Figure 3: Depth profile of the magnetic susceptibility (k) in a pasture area 10 km east of the metallurgical factory.**

Three 1 $m^2$ reference sites within commonly present land uses in the region, i.e. arable land (51°11'0.66", 3°50'9.12"), forest (51°10'54.16", 3°50'22.63") and pasture (51°10'39.56", 3°50'2.02"), were selected downwind of the metallurgical factory to investigate the small-scale magnetic soil variability (Figure 1B). All sites were located on the coversand ridge in uniform geological conditions[75] and pedologically, an arenosol had developed in the arable land, while the forest and pasture site were characterized by a podzol and a gleyic phaeozem, respectively.[76] The soil in the arable land had been disturbed over the years by ploughing and other soil tillage operations, resulting in a homogeneous soil down to the ploughing depth. The forest, which was a moorland until the 18th century, had been reforested with conifers for the last time between 1920 and 1980.[77] It was dominated by *Pinus nigra* sp. *laricio*, *Pinus sylvestris* and *Picea abies*, occupying respectively 73.2, 26.6 and 0.2% of the surface. No shrub layer was present, but the soil was generously covered with mosses. Although the forest was publicly accessible, the soil remained undisturbed as the sampling site was located far from walking

trails. In a previous study, high magnetic susceptibility was observed in the forest, with increasing values towards the metallurgical factory (Figure 1B, Appendix A).[62] The pasture soil, having been under cultivation for two seasons in 2011-2012, was situated in a wetland where soil motion (primarily due to cattle trampling) has strongly influenced its properties.

Additional to the investigation of reference sites, magnetic measurements were carried out every 100 m along four 1800 m long transects east of the metallurgical factory to investigate large-scale magnetic patterns (Figure 1C). The 72 measurement points covered six different land uses: forest (31), arable land (13 in maize fields and 1 in fallow field), pasture (9), moorland (3), anthropogenic (6 in private gardens and 8 on roadsides) and bare dunes (1). All soils were equally located on diamagnetic, sandy substrates and some of them have been altered due to human activity.

## 2.2 Soil surface magnetic susceptibility

The influence of soil cover and local surface variability on the topsoil magnetic signal was investigated to establish a robust protocol for susceptibility mapping in different land use classes. Within the 1 $m^2$ reference sites in arable land, forest and pasture, topsoil magnetic susceptibility was measured through 36 non-overlapping records in a 6 x 6 cell grid using a MS2D loop sensor (Bartington Instruments Ltd., UK). This sensor, with a 185 mm loop size and a known penetration depth of 8 cm, integrates magnetic variation within a 4300 $cm^3$ sampling volume.[47] The instrument was air-calibrated prior to each recording. Measurements were first performed on the undisturbed surface, after which vegetation or litter was manually removed and topsoil susceptibility recording was repeated. Statistical hypothesis testing with nine paired-sample t-tests was applied to check for significant differences in magnetic susceptibility values between measurements made above and underneath plant cover, for the three land use classes considered (Appendix B).

## 2.3 Magnetic depth profiling

To corroborate the relationship between topsoil susceptibility values and the associated magnetic soil profile, undisturbed core samples were taken at nine grid points within the 1 m² reference sites to a depth of 40 cm by hammering a plastic tube into the soil. Split cores were scanned every 2 mm with a MS2E sensor (Bartington Instruments Ltd., UK) which is most sensitive to the underlying surface area of 3.8 mm x 10.5 mm and down to 3.5 mm depth. One split core at each site was subsampled every 3 cm and the remaining cores were subsampled at the bottom and the top of the core. Low- and high-frequency volumetric magnetic susceptibility ($k_{lf}$ and $k_{hf}$) were measured on the subsamples with a MS2B dual frequency sensor (Bartington Instruments Ltd., UK) at 0.465 and 4.65 kHz, respectively. The susceptibilities were then divided by the samples' densities (ρ) in order to obtain their mass-specific susceptibilities ($X_{lf}$ and $X_{hf}$). Subsequently, scanning electron microscopy (SEM) analysis was done in combination with energy dispersive X-ray detection (EDX) (Quanta 250, FEI, USA). In addition, anhysteretic remanent magnetization (ARM) was measured using a LDA5/PAM1 magnetizer (AGICO, Czech Republic) with a steady field of 500 µT and an alternating field of 200 mT in combination with a JR-6 magnetometer (AGICO, Czech Republic). The ARM susceptibility ($X_{ARM}$) was determined as the ratio of the ARM to the steady field. To calculate ARM/SIRM ratios, the samples were magnetically saturated in a pulse magnetizer (Molspin Ltd, UK) at 1 T and their saturated isothermal remanent magnetization (SIRM) was measured in the JR-6 magnetometer. Afterwards, a backfield of 300 mT was immediately applied to the samples in the pulse magnetizer and their subsequent isothermal remanent magnetization ($IRM_{-300}$) was measured in the JR-6 magnetometer. The S-ratios of the samples were then calculated as $\text{S-ratio} = \frac{IRM_{-300}}{SIRM}$. Lastly, all samples were analysed in a J-coercivity meter[45, 78, 79] to obtain their saturation magnetization ($M_s$), saturation remanence ($M_{rs}$) and relative decay viscosity coefficient ($S_d$). The concentration of trace elements was measured in all samples. As Cd, Pb and As are toxic for living

organisms, and even essential (Mn, Fe, Zn, Cu) or useful (Co, Cr, Ni) elements become harmful when they are bio-available in the soil or groundwater in high concentrations,[80] all these elements were selected for extraction by aqua regia[81] and subsequent inductively coupled plasma optical emission spectrometry (ICP-OES) (American Assay Labs, USA). The Pollution Load Index (PLI)[82] was calculated for each subsample (i) in each land use class (j) based on each measured trace metal concentration (n) according to

$$PLI_{i,j} = \sqrt[n]{CF_{1,i,j} \times CF_{2,i,j} \times \ldots \times CF_{n,i,j}}$$

where $CF_{n,i,j}$ is the contamination factor of trace metal n calculated as

$$CF_{n,i,j} = \frac{concentration_{n,i,j}}{min(concentration_{n,j})}.$$

Beside the core loggings, a MS2H downhole sensor (Bartington Instruments Ltd., UK) was used in the field to record the magnetic susceptibility below 40 cm. As the operating frequencies of the MS2H (1.3 kHz) and MS2E (2.0 kHz) sensors are comparable, collected data from both sensors can be evaluated together. In addition, the operating frequencies did not influence the susceptibility measurements as superparamagnetic (SP) particles were absent at all sites.

To investigate how soil properties influence the dispersal of magnetic particles through soil, Kopecky ring samples were taken down to a depth of 25 cm in the arable land, forest and pasture, each time at two locations within the reference site. We calculated the volumetric water content (θ) and soil bulk density (ρ),[83] and determined soil texture through the pipette method[84] alongside the organic carbon (OC) content[85] and soil pH-KCl.[86] The $CaCO_3$ content was determined by adding excess $H_2SO_4$ followed by back titration with NaOH.[87] For subsequent analysis, the results were averaged over the two locations within the sites. At each site, profile descriptions were made based on Dutch auger sampling.

# 3. Results and discussion

## 3.1 Local magnetic variability influenced by land use

### *3.1.1 Soil surface magnetic susceptibility*

The mean topsoil susceptibilities differed significantly between all three reference sites, both when measured above and underneath plant cover (Appendix B, Figure 4). Highest values were found in the forest where the canopy and undisturbed soil allowed for a long-term preservation of the soil magnetic signature. The values are similar to the results in Figure 1B and characteristic for industrial areas.[11, 24, 33, 38, 65] Susceptibility was lowest in the arable land, while intermediate values were obtained in the pasture. The coefficient of variation underneath the plant cover was slightly larger in the pasture (0.14) than in the arable land (0.11) and forest (0.11), suggesting more small-scale magnetic variability. This might be related to the wet pasture soil being more prone to topsoil modification, e.g. cattle trampling, and the lack of homogenization by ploughing. The number of random records necessary to reliably capture this variability in an average value was determined through iterative sample size calculations following Webster and Lark (2013).[88] Assuming a confidence level of 5% and a tolerated deviation of 10% from the true mean, a minimum of 10 topsoil records per m² were required for pasture, while 8 measurements sufficed for arable land and forest. We decided to use 10 records as general guideline for further analysis.

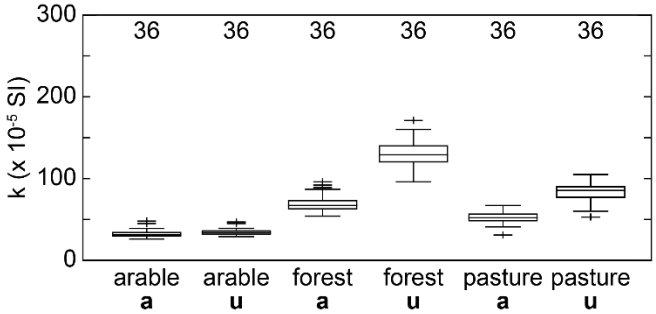


**Figure 4: Boxplots of topsoil susceptibility (k) for each land use class, both as measured above (a) and underneath (u) plant cover. The whiskers correspond to the most extreme data points which are not outliers and the crosses correspond to extreme values considered as outliers (> 1.5 x interquartile range[89]). The number of records for each land use class is given on top of the figure.**

In the forest and pasture, magnetic susceptibility was 61 ± 4 and 31 ± 4 x $10^{-5}$ SI higher when measured underneath the plant cover compared to the values obtained above this layer (Figure 4). In the arable land, the susceptibility only increased by 2 ± 1 x $10^{-5}$ SI underneath plant cover because the cereal field had just been harvested and hence plant cover was very thin. In relative terms, the susceptibility decreased by 6, 47 and 37% in arable land, forest and pasture when measured above plant cover, which is similar to previous results in forests: Magiera et al. (2016)[24] and prior research[62] in the forest reference site reported decreases of 37% (19 x $10^{-5}$ SI) and 32% (47 x $10^{-5}$ SI). The lower values above plant cover are due to the diamagnetic properties of the organic material and to large air spaces in the vegetation and litter that dilute the magnetic signal. Thus, plant cover should be removed before measuring topsoil magnetic susceptibility to reduce the magnetic surface variability caused by differences in plant cover and to obtain an even soil surface for recording.

### *3.1.2 Magnetic depth profiling*

#### *3.1.2.1 Forest*

The forest podsol features an acid, organic topsoil that covers an illuvial B horizon on top of a sandy substrate (Figures 5 and 6). The last is known to be poor in iron and contains no primary magnetic minerals sensu lato, but is dominated by diamagnetic minerals as corroborated by the negative susceptibility values in the B and BC horizon. Yet, a small amount of Fe ions is released from the parent material during weathering. As acid, organic topsoils generally favour the transformation of Fe ions into weakly crystalline iron (oxy)hydroxides (e.g. ferrihydrite),[74] slightly enhanced magnetic responses are naturally found in organic topsoils. The latter also promote the formation of iron-organic complexes which are then leached into the B horizon where other magnetic minerals (e.g. goethite) can be formed. The S-ratio in the B horizon pointed to an enhancement of hard magnetic particles, however, as the magnetic susceptibility dropped below 1 x $10^{-5}$ SI in this layer (Figure 5), the diamagnetic fraction masks most of the magnetic response of the few secondary magnetic minerals present. For all subsamples in

the soil profile, $X_{lf}$ equalled $X_{hf}$ and the pattern of $X_{lf}$ was similar to the SIRM pattern (data not shown), so superparamagnetic (SP) particles were not formed or have been dissolved in the acidic soil conditions.[74, 90] Although highest susceptibility values were found in the organic A horizon, the upper part of the AB horizon also showed magnetic enhancement. According to the S-ratio, this horizon is marked by an increased influence of soft magnetic particles, compared to the B horizon. The effect is continued in the A horizon where the magnetic response was fully dominated by soft magnetic minerals. As MD particles often have an anthropogenic origin,[72] we assume that coarse magnetite or maghemite particles have been deposited onto the soil and were transported into the A and AB horizon. Pedogenic iron (oxy)hydroxides might have been formed in the A horizon, but the increased ARM/SIRM ratio rather reflects the presence of viscous grains below 7.5 cm as the viscosity coefficient ($S_d$) increased towards the bottom of the profile (from ~4 x $10^{-3}$ to ~12 x $10^{-3}$). The magnetic response in the A horizon is dominated by the anthropogenic enrichment of MD particles. This is evidenced by SEM photographs of the organic soil layers which showed large, spherical magnetic particles known to be present in combustion exhaust (Figure 7).[91] Low (~0.06) $M_{rs}/M_s$ ratios in the upper 13 cm further confirm the deposition of MD grains on the soil surface, as well as the comparison of the subsamples' $X_{ARM}$ (0.66 – 0.83 x $10^{-3}$) and $k_{lf}$ (0.48 – 0.61 x $10^{-3}$ SI) in the King plot (data not shown).[45, 92] In addition, trace metal concentrations reached peak values in the O/A horizon except for Al, which is an indication of podsolisation of the soil profile (Figure 5). Strongly positive correlations ($r > 0.90$) were also found between the low-frequency soil magnetic susceptibility and trace metal concentrations (except for Al and As) in the soil core subsamples (Table 1), demonstrating the suitability of soil magnetic susceptibility as a proxy for airborne pollution.[80, 91]

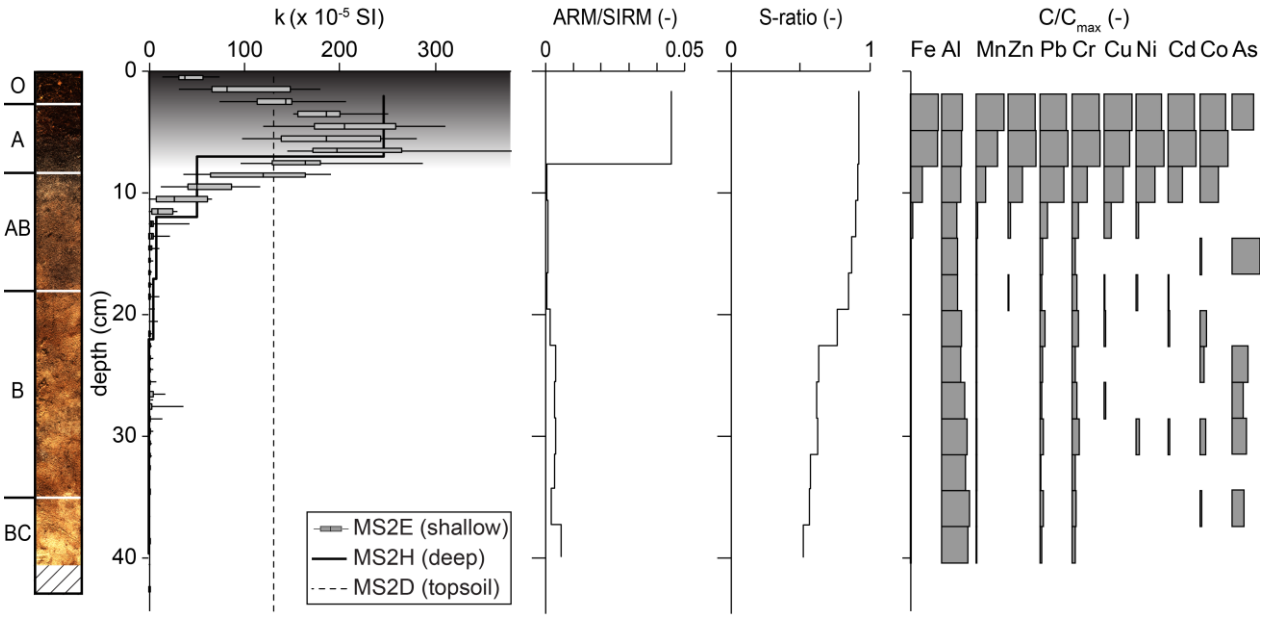


**Figure 5: Photograph of the analyzed forest soil core and accompanying depth profile of k, the ARM/SIRM ratio, S-ratio and relative enrichments of trace metals in the soil. No hysteresis parameters are shown because a high coercivity component is present within the profile. *Photograph:* O = organic horizon, A = humic, mineral horizon, AB = transition zone between A and B horizon, B = illuvial horizon, BC = transition zone between B and C horizon. *Susceptibility profile:* A MS2E sensor was used to scan the nine sampled soil cores (depth < 42 cm) and the nine records at each depth were combined into one boxplot. The whiskers correspond to the minimum and maximum values. A MS2H sensor was used in the field (depth < 75 cm) to establish the susceptibility profile at greater depths. The mean topsoil magnetic susceptibility as measured with the MS2D sensor is also plotted through the entire profile; the shaded, grey area represents the decreasing depth sensitivity of this sensor when placed on top of the soil.[47] *Relative enrichment profiles:* The relative enrichment of trace metals was calculated for each depth as the subsample's metal concentration divided by the maximum metal concentration in the entire profile. The x-axis scale ranges from 0 to 1 for each metal.**

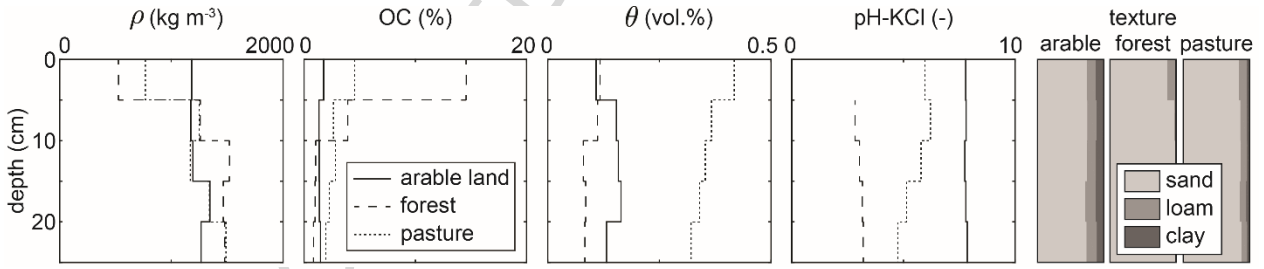


**Figure 6: Depth profiles of physical soil properties in the arable land, forest and pasture. ρ = soil bulk density, OC = organic carbon content, θ = volumetric water content. The x-axis scales for the texture profiles ranges from 0 to 100%. The pH in the upper forest layer could not be determined due to the small amount of soil material in the sample. Additional measurements showed that the OC content in the pasture remained low (1.5 - 2.0%) between 30 and 35 cm.**

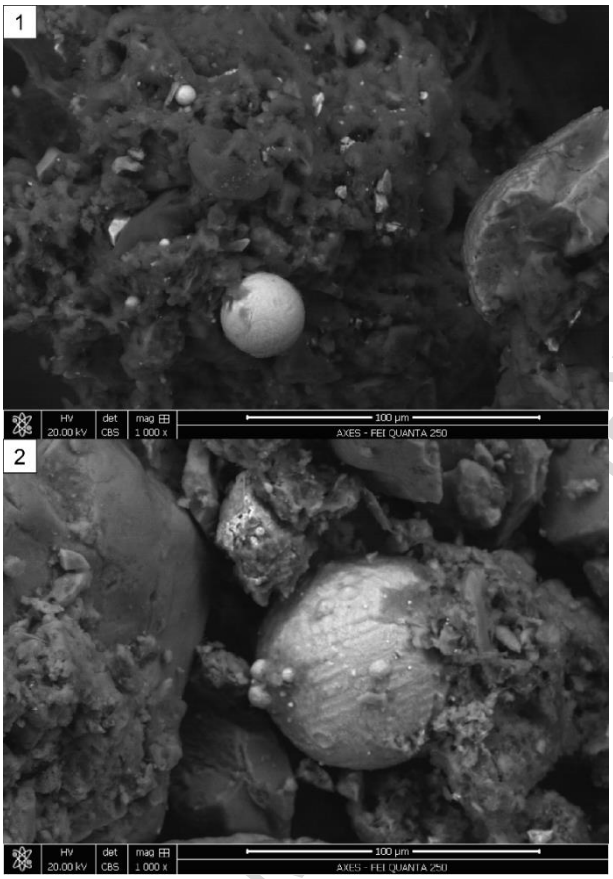


**Figure 7: SEM photographs of the soil in the upper 15 cm of the forest (1) and pasture (2). The white spherules are probably combustion-related particles. Magnification: 1000x, scale: 100 µm.**

**Table 1: Pearson correlation coefficients between the low-frequency magnetic susceptibility ($X_{lf}$) of the soil core subsamples in forest and pasture as measured with the MS2B dual frequency sensor, and their concentrations of hazardous soil elements and Pollution Load Index (PLI). Only samples with concentrations above the detection limit were used for calculating the correlation coefficients and their number is given inside brackets. Correlations in arable land were not meaningful due to a restricted sampling range.**

| | forest | | pasture | |
|---|---|---|---|---|
| Al | -0.13 | (22) | -0.24 | (29) |
| As | -0.02 | (8) | 0.05 | (24) |
| Cd | 0.92* | (14) | 0.72* | (29) |
| Co | 0.96* | (16) | 0.58* | (28) |
| Cr | 0.95* | (22) | 0.66* | (29) |
| Cu | 0.94* | (16) | 0.62* | (29) |
| Fe | 0.96* | (22) | 0.82* | (29) |
| Mn | 0.92* | (22) | 0.78* | (29) |
| Ni | 0.95* | (14) | 0.46* | (29) |

| | | | | |
|---|---|---|---|---|
| Pb | 0.90[(b)] | (21) | 0.39[(b)] | (29) |
| Zn | 0.92[(b)] | (13) | 0.85[(b)] | (27) |
| PLI | 0.97[(b)] | (22) | 0.81[(b)] | (29) |

[*] significant correlation (5% level)

*3.1.2.2 Pasture*

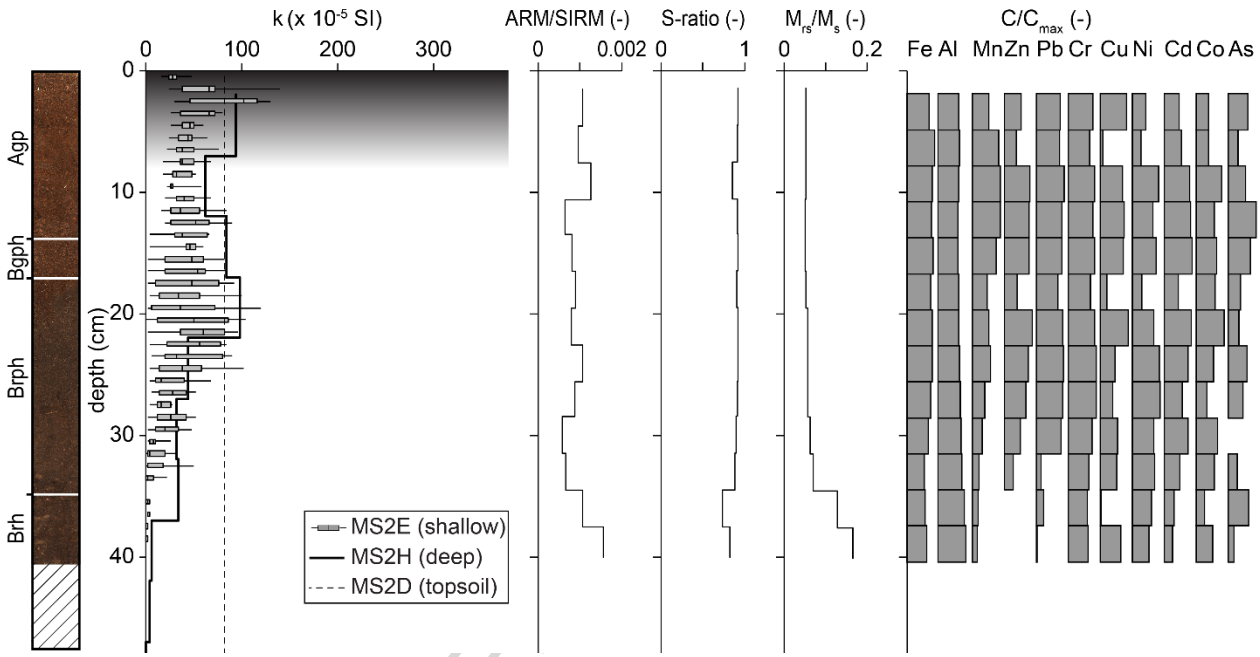


**Figure 8: Photograph of the analyzed pasture soil core and accompanying depth profile of k, the ARM/SIRM ratio, S-ratio, $M_{rs}/M_s$ ratio and relative enrichments of trace metals in the soil. *Photograph:* Agp = humic, mineral horizon with gley features and which has been ploughed in 2011 – 2012 (see *2.1 Study area*), Bgph = humic, illuvial horizon with gley features and which has been ploughed in 2011 – 2012 (see *2.1 Study area*), Brph = humic, reduced, illuvial horizon which has been ploughed in 2011 – 2012 (see *2.1 Study area*), Brh = humic, reduced, illuvial horizon. *Susceptibility profile:* A MS2E sensor was used to scan the nine sampled soil cores (depth < 42 cm) and the nine records at each depth were combined into one boxplot. The whiskers correspond to the minimum and maximum values. A MS2H sensor was used in the field (depth < 75 cm) to establish the susceptibility profile at greater depths. The mean topsoil magnetic susceptibility as measured with the MS2D sensor is also plotted through the entire profile and the grey area represents the signal penetration depth of this sensor when placed on top of the soil.[47] *Relative enrichment profiles:* The relative enrichment of trace metals was calculated for each depth as the subsample's metal concentration divided by the maximum metal concentration in the entire profile. The x-axis scale ranges from 0 to 1 for each metal.**

The phaeozem profile that developed in the pasture is marked by a thick, humus rich organic layer (Figures 8 and 6). The profile is situated in a small depression which explains its high moisture content. Intense leaching has removed $CaCO_3$ from the profile, which is also reflected in the slightly acid pH. Reduced Mn ions might have been oxidized in the upper horizons affected by gley, and as the OC content is not extremely high, we assume that subsequent leaching of Mn oxides has darkened the soil.

Considering $X_{lf}$ equalled $X_{hf}$ in all soil core subsamples, the presence of pedogenic SP particles is not indicated. Thus, SP ultrafine particles have not been formed or have been dissolved. However, formation of fine SD grains out of weathered Fe ions from the parent material cannot be excluded. In general, alternating oxidising and reducing conditions in the upper, organic rich Agp and Bgph soil horizons favour the formation of strong magnetic particles[74, 93] which might subsequently be leached into the B horizon. The S-ratio is rather constant along the profile and close to unity, indicating the overall dominance of ferrimagnetic minerals. The ARM/SIRM ratio is about one order of magnitude lower compared to the A horizon of the forest profile, suggesting coarser ferrimagnetic particles in the pasture profile. Only in the Brh horizon, the S-ratio is slightly decreased, and the $M_{rs}/M_s$ and ARM/SIRM ratios are enhanced, indicating a mixture of soft and hard SD particles of pedogenic origin. We hypothesize that anthropogenic, soft MD particles and heavy metals have been deposited onto the soil and were subsequently mixed within the ploughing layer when the pasture field was under agricultural use (2011 – 2012). This can explain the enhanced magnetic susceptibility and the decreased $M_{rs}/M_s$ ratio within the upper 35 cm, along with the rather homogeneous distribution of heavy metal concentrations compared to the forest profile. When the field then again was used as pasture, atmospheric deposition of magnetic particles re-established the top-down accumulation of magnetic particles and heavy metals, with slightly higher susceptibility values in the upper 20 cm as a result. Except for Al, As, Ni and Pb, high correlations ($r > 0.50$) were again found between the low-frequency soil magnetic susceptibility and trace metal concentrations (Table 1), suggesting that the magnetic properties are dominated by anthropogenic particles.

*3.1.2.3 Arable land*

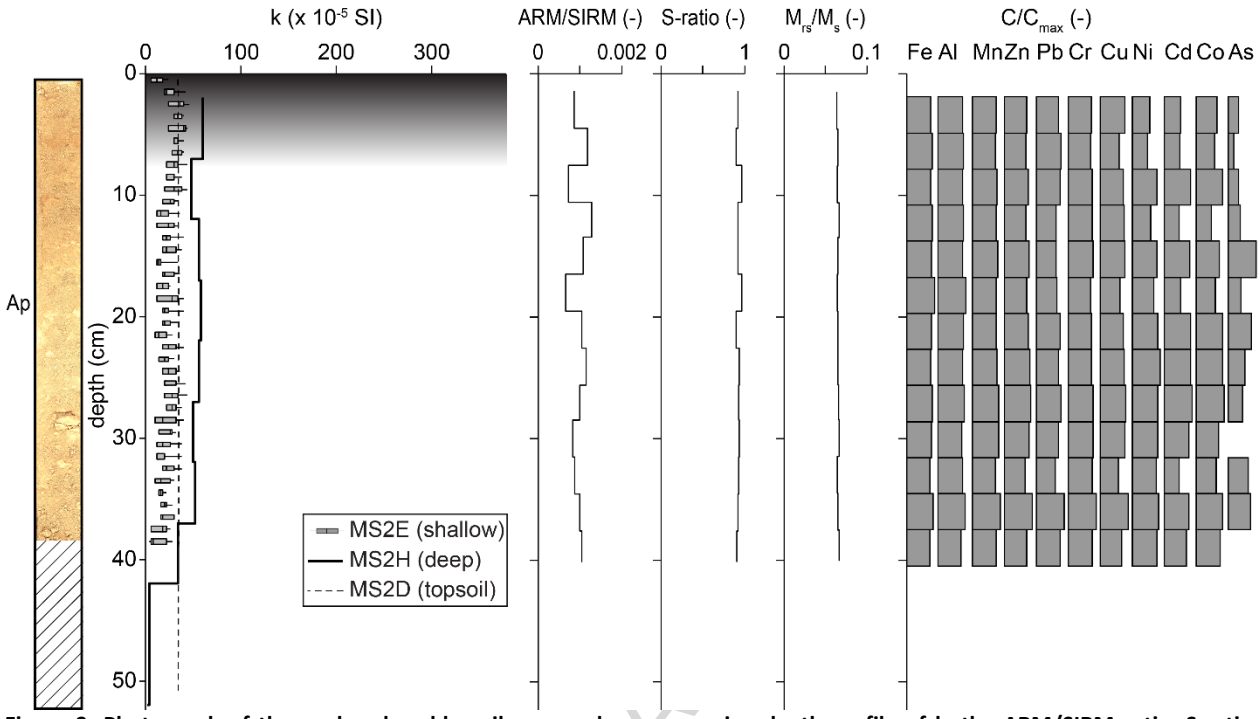


**Figure 9: Photograph of the analyzed arable soil core and accompanying depth profile of k, the ARM/SIRM ratio, S-ratio, $M_{rs}/M_s$ ratio and relative enrichments of trace metals in the soil. *Photograph:* Ap = humic, mineral horizon which has been ploughed. *Susceptibility profile:* A MS2E sensor was used to scan the nine sampled soil cores (depth < 42 cm) and the nine records at each depth were combined into one boxplot. The whiskers correspond to the minimum and maximum values. A MS2H sensor was used in the field (depth < 75 cm) to establish the susceptibility profile at greater depths. The mean topsoil magnetic susceptibility as measured with the MS2D sensor is also plotted through the entire profile and the grey area represents the signal penetration depth of this sensor when placed on top of the soil.[47] *Relative enrichment profiles:* The relative enrichment of trace metals was calculated for each depth as the subsample's metal concentration divided by the maximum metal concentration in the entire profile. The x-axis scale ranges from 0 to 1 for each metal.**

As the arenosol in the arable land is poorly developed and has a low OC content (Figure 6), we assume that only a limited amount of pedogenic magnetic particles have been formed within the profile. In addition, the background magnetic response in this profile is diluted by high $CaCO_3$ contents. Low pedogenic enhancement is inferior to the presence of anthropogenic MD particles which are mixed homogeneously within the plough layer. The magnetic susceptibility was enhanced in the upper 42 cm and dropped to 4 x $10^{-5}$ SI below this depth, where pedogenic formation of magnetic particles might become more important compared to the upper soil layers (Figure 9). As $X_{lf}$ equalled $X_{hf}$ in all soil core subsamples, no indications of SP particle presence were found. The S-ratio is almost constant compared to the forest profile, indicating the absence of high coercivity minerals such as goethite. The low $M_{rs}/M_s$

ratio (< 0.1) along the entire profile and the distribution of trace metals in the plough layer showed that anthropogenic MD particles and trace metals are evenly spread in this layer. Although the susceptibility profile in arable land was similar to the PLI profile (data not shown), correlations between the low-frequency magnetic susceptibility and trace metal concentrations in the arable land were not meaningful due to a restricted sampling range.

*3.1.2.4 Magnetic profiling over different land use classes*

Similar to previous research,[20, 22, 91] strong correlations between the soil magnetic susceptibility and trace metal concentrations along with a minor contribution of pedogenically formed magnetic particles showed that soil magnetic susceptibility can be used as a proxy for airborne pollution in different land use classes. Analogous to the topsoil results in each land use class (see section *3.1.1*), highest magnetic susceptibility values were recorded in the forest profile, followed by the pasture and arable land. The forest canopy efficiently intercepts airborne pollution and magnetic particles are easily adhered on humic matter within the organic soil layers. The undisturbed layering of soil horizons prevents the downward migration of anthropogenic magnetic particles and causes a magnetic enhancement in the uppermost soil horizon. In the arable land, captured particles are partly removed when harvesting crops and partly diluted in the soil profile due to ploughing. The intermediate values in the pasture likely relate to the accumulation of recently deposited particles together with particles already present within a former plough layer. These results show how land use strongly influences the distribution of magnetic particles through the soil profile and explain why magnetic susceptibility in the reference sites did not correlate with the distance to the pollution source. The highest susceptibility values were found in the forest located 1700 m from the factory's chimney, while intermediate and lowest values were obtained in the pasture and arable land located at 1300 m and 1500 m from the source. At all reference sites, susceptibility almost decreased to zero when reaching the C horizon (Figures 5, 8 and 9), reflecting the dominance of the diamagnetic parent material in bulk measurements of susceptibility. Due to conditions

favoring the pedogenic formation of magnetic particles and the formation of organic – iron oxide complexes in the upper, organic soil layers, enhanced magnetic properties in all profiles related to high contents of organic material (Figures 5, 6, 8 and 9). Although the reference sites are located in a sandy soil environment, it was assumed that leaching of magnetic particles is limited where organic soil horizons are present.

## 3.2 Regional magnetic prospection over different land use classes

### *3.2.1 Soil surface magnetic susceptibility*

Following the recommendations developed in section *3.1.1*, plant cover was removed over 1 m² at each of the 72 transect points (Figure 1C) prior to recording ten randomly placed topsoil susceptibility measurements on this m² with a MS2D loop sensor (Bartington Instruments Ltd., UK), retaining their mean for further analysis. Six different land use classes were recorded over the 72 transect points (see section *2.1*). Except for three extreme values in the anthropogenic class, the highest values were obtained in forests where magnetic susceptibility up to 187 x $10^{-5}$ SI was recorded (Figures 10 and 11). Polluting particles are blown over the entire study area and the forest canopy acts as a shield catching windblown magnetic particles, which are then preserved in the organic soil layers. Lower values were obtained in the other land use classes where no high canopy is present or was removed and where land was subject to anthropogenic modifications (e.g. ploughing and harvesting). Average soil magnetic susceptibility reached 39, 55, 60 and 63 x $10^{-5}$ SI in arable land, pasture, bare soil and moorland. The magnetic enrichment in anthropogenic soils can be attributed to local human activity such as traffic exhaust next to roads, private dumps and burning. Consistent with the observations at the reference sites, the lowest and most homogeneous values were recorded in arable land, while slightly increased and more variable susceptibility values were observed in pasture and moorland. According to aerial photographs dating from 2000,[94] site A on Figure 11 was used for waste disposal in the past, sites B have been variously cultivated between 2000 and 2013 and trees have been removed from site C in 2008.

Since the land use history strongly influences the distribution of magnetic particles through soil, straightforward interpretation of magnetic topsoil records is difficult and no unambiguous conclusions can be made about the airborne pollution impact. Highest susceptibility values in the forest might be related to its capacity for capturing and retaining airborne particles, rather than reflecting a general trend of decreasing PM concentration with increasing distance from the factory. Likewise, low susceptibility values in arable land can be attributed to dilution of magnetic particles within the ploughing layer, instead of to a decreasing PM trend. If such a trend would fully dominate the susceptibility records, values in arable land closest to the factory should be higher than values in arable land further away, or even surpass the susceptibility records in the forest.

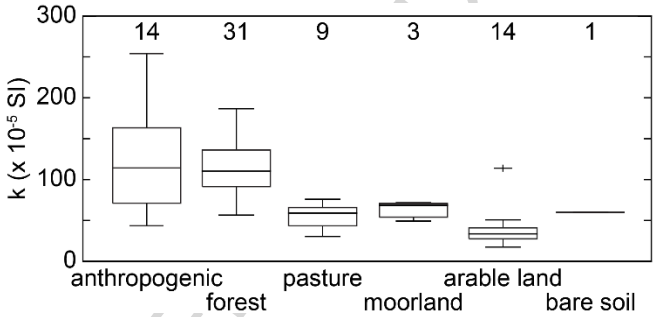


**Figure 10: Boxplots of mean topsoil susceptibility (k) after removal of plant cover for each land use class. The whiskers correspond to the most extreme data points which are not outliers and the crosses correspond to extreme values considered as outliers (> 1.5 x interquartile range[89]). The number of records for each land use class is given on top of the figure.**

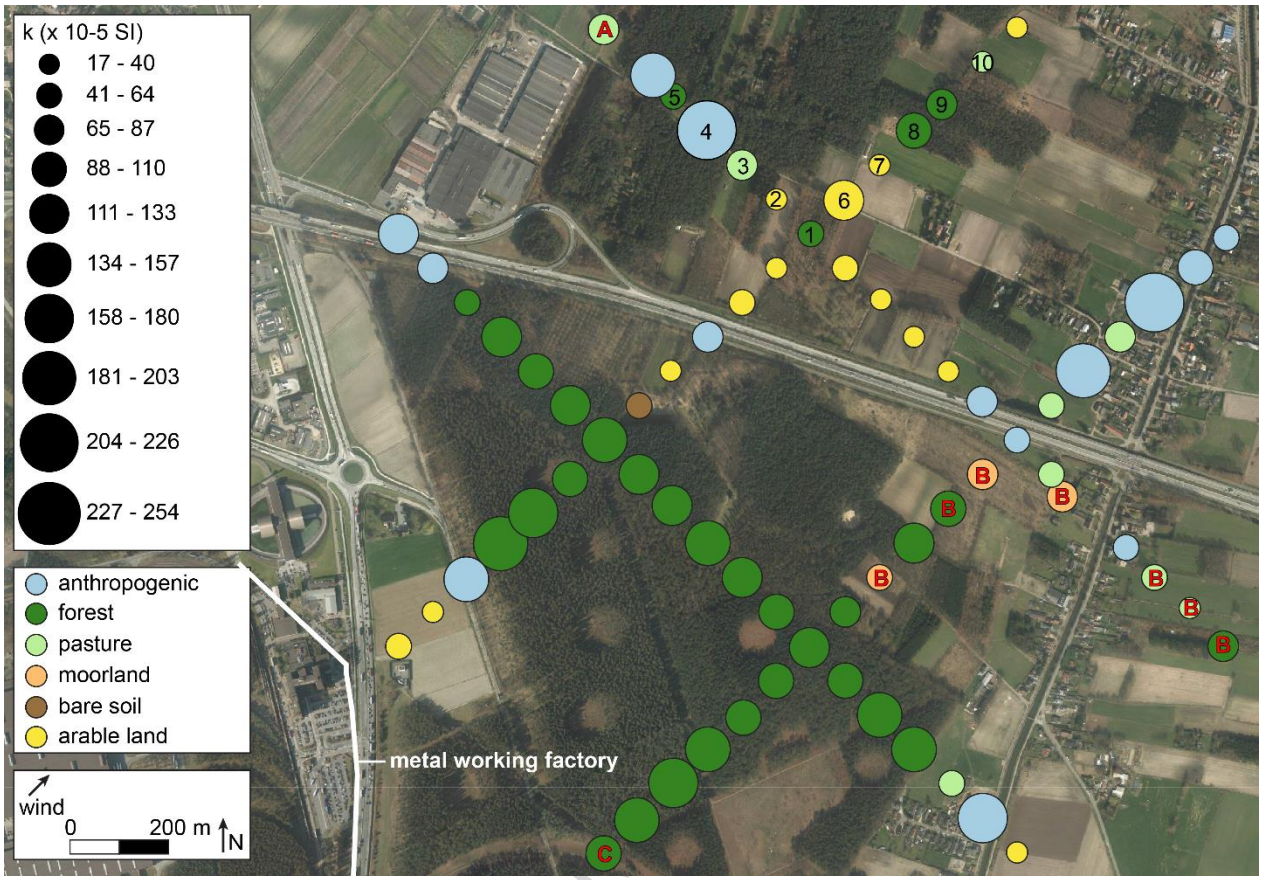


**Figure 11: Distribution of topsoil susceptibility (k) along the transects. Different colors are appointed to different land uses and the size of the dots is proportional to the topsoil susceptibility. At a subset of 10 grid points (numbers 1 – 10), soil cores were taken and analyzed down to a depth of 40 cm. Site A has been prone to dumping activities in the past, sites B have been variously cultivated between 2000 and 2013 and site C has been grubbed in 2008.**

### *3.2.2 Magnetic depth profiling*

Large-scale magnetic depth variability was investigated by analyzing 10 soil cores in the transects (Figure 11, cores 1-10) analogous to section *2.3*. The forest soils (cores 1, 5, 8 and 9) mostly displayed a peak in the O and A horizons along with pedogenic or anthropogenic enhancement in deeper layers (Figure 12). However, profile 1, obtained in a forested area with low tree density but with shrubs and grasses, showed a different pattern. Land use history seems to influence the current magnetic soil signature as aerial photographs have shown that the area was under pasture until 2003.[94] The anthropogenic profile (core 4) revealed very high (up to 1541 x $10^{-5}$ SI) and variable records due to intense anthropogenic interference, whereby the soil was excavated for sand extraction (personal communication with the land owner). At both pasture soils (cores 3 and 10), the profile displayed slightly enhanced yet rather constant

magnetic values, which might be due to pedogenic formation of magnetic particles, following the accumulation and migration of magnetic particles through soil or related to an old plough layer as – according to aerial photographs[94] – profile 10 has been under cultivation in 2014. The magnetic records were also enhanced but constant over the entire plough layer in the arable soils (cores 2, 6 and 7). A piece of metal was visually observed in core 6, explaining the outlier (753 x $10^{-5}$ SI) at 14.6 cm depth. The strong magnetic enhancement in this entire profile might be related to differences in phytosanitary treatment or tillage techniques because, unlike the other arable soils (cores 2 and 7), this soil (core 6) was not planted with corn during the present study. These results show that magnetic depth profiles in the study area are strongly influenced by the land use history and only to a minor extent by pedogenic formation of magnetic particles. As topsoil susceptibility sensors only record the upper 8 cm of the soil,[47] unravelling the impact of pollution using topsoil magnetism is far from straightforward without prior knowledge about land use.

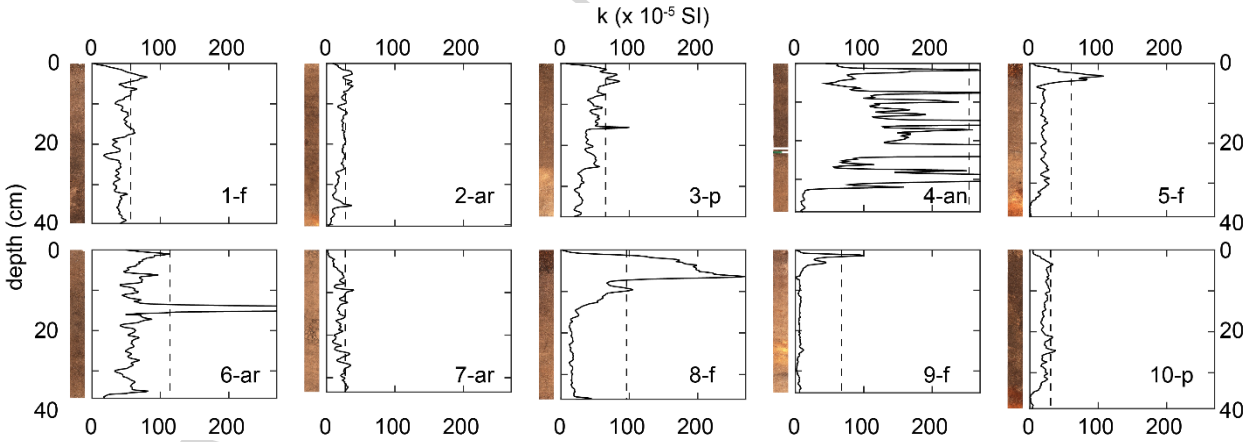


**Figure 12: Susceptibility (k) depth profiles as measured with the MS2E sensor and photographs of 10 soil cores which are located in the northern part of the study area (Figure 11, cores 1-10). The mean topsoil magnetic susceptibility (k) as measured with the MS2D loop sensor is also plotted through the entire profile (vertical dashed line). The land use class is also given: f = forest, ar = arable land, p = pasture and an = anthropogenic.**

All split cores were subsampled at the bottom and the top of the core for the chemical analyses described in section *2.3*. Moderate to strong correlations were obtained between the low-frequency magnetic susceptibility in the soil core subsamples and their concentrations of hazardous soil elements (Table 2). Although the values for Pb (0.79), Ni (0.59) and the PLI (0.53) are of environmental importance,

the correlations are generally lower than for the small-scale reference sites (Table 1). The magnetic footprint which reflects atmospheric deposition of magnetic particles and associated trace metals might be dominated by the application of livestock manure, inorganic fertilizers, industrial waste (e.g. byproducts from the food industry and paper or textile production) and sewage sludge to the soil.[95, 96] Private garden works and other soil tillage might further alter the distribution of metals in soils, leading to poorer correlations between the magnetic susceptibility and the considered metals in the soils.

**Table 2: Pearson correlation coefficients between the low-frequency magnetic susceptibility ($X_{lf}$) of the subsamples in the 10 soil cores of the transect (Figure 11, cores 1-10) as measured with the MS2B dual frequency sensor, and their concentrations of hazardous soil elements and Pollution Load Index (PLI). Only samples with concentrations above the detection limit were used for calculating the correlation coefficients and their number is given inside brackets.**

| element | correlation | |
|---|---|---|
| Al | - 0.47* | (20) |
| As[(a)] | - | - |
| Cd | - | (0) |
| Co | 0.40 | (20) |
| Cr | 0.32 | (20) |
| Cu | 0.40 | (19) |
| Fe | 0.93* | (20) |
| Mn | 0.36 | (20) |
| Ni | 0.59* | (18) |
| Pb | 0.79* | (20) |
| Zn | -0.35 | (4) |
| PLI | 0.53* | (20) |

* significant correlation (5% level)
[(a)] Concentrations for As could not be calculated due to an error in the ICP-OES device.

# 4. Conclusion

Detailed analysis of local magnetic variability and trace metal concentrations in soils across different land-use classes (arable land, forest and pasture) showed the persisting dominant impact of atmospheric

PM deposition on the soil magnetic response. However, as different PM deposition and migration processes influenced the distribution of magnetic particles down the soil profile, topsoil records could not be interpreted unambiguously for describing the impact of pollution across the wider area. Hereby, the strong influence of land use on the subsurface distribution of magnetic particles disturbed the correlation between the magnetic signal at the reference sites and their distance to the pollution source. Additional downhole susceptibility sounding revealed a dispersion of magnetic particles throughout the soil profile, facilitating interpretation of the local topsoil variability and providing insight into the impact of land use. Still, these integrated topsoil and downhole magnetic records did not enable discriminating pollution trends over the wider area. Although our data show the limitations of topsoil magnetic pollution mapping across land use classes, the reliability of targeting isolated land use classes (such as arable land and pasture) in heterogeneously used regions remains to be evaluated. Here, the integration of complementary analytical methods such as SEM or elemental analyses can provide additional support for relating the magnetic response to pollution.

# 5. Appendices

## 5.1 Appendix A – Prior research in the forest reference site

Topsoil susceptibility was measured in the forest reference site in 2015 using a MS2D loop sensor (Bartington Instruments Ltd., UK) at 120 locations in the forest, which were selected partly random and partly on a regular 100 m grid, with at least 25 m spacing. After litter removal, ten magnetic susceptibility records were taken randomly in a square meter at each location. Median values were then used to produce an interpolated susceptibility map with ordinary kriging. High magnetic susceptibility was observed in the forest, with increasing values towards the metallurgical factory (Figure 1B).[62]

## 5.2 Appendix B – Statistical hypothesis testing between arable land, forest and pasture

Nine paired-sample t-tests ($\alpha = 0.05$) were executed to reveal significant differences in magnetic susceptibility between arable land, forest and pasture (Table B.1). The mean topsoil susceptibilities differed significantly between all three reference sites, both when measured above and underneath plant cover ($p < 0.05$ for all tests).

**Table B.1: P-values for each of the nine paired-sample t-tests.**

| t-tests between values underneath and above **plant cover** | | t-tests between different **land use** classes | | | |
|---|---|---|---|---|---|
| | | | forest | arable land | pasture |
| forest | $1.69 \times 10^{-28}$ | forest | | $1.52 \times 10^{-21}$ (b) | $5.57 \times 10^{-10}$ (b) |
| arable land | $2.54 \times 10^{-5}$ | arable land | $1.78 \times 10^{-30}$ (a) | | $2.53 \times 10^{-18}$ (b) |
| pasture | $7.11 \times 10^{-16}$ | pasture | $1.65 \times 10^{-14}$ (a) | $1.35 \times 10^{-22}$ (a) | |

(a) underneath plant cover
(b) above plant cover

# 6. Funding

This work was supported by the Research Foundation Flanders (FWO). Y.D. and A.C. receive a doctoral fellowship grant (grant numbers 1S33417N and 1S15122716N). P.D.S. receives a postdoctoral fellowship grant (grant number 1288117N).

# 7. References

1. Morton-Bermea, O.; Hernandez, E.; Martinez-Pichardo, E.; Soler-Arechalde, A. M.; Lozano Santa-Cruz, R.; Gonzalez-Hernandez, G.; Beramendi-Orosco, L.; Urrutia-Fucugauchi, J., Mexico City topsoils: Heavy metals vs. magnetic susceptibility. *Geoderma* **2009,** *151*, 121-125.

2. Kardel, F.; Wuyts, K.; Maher, B. A.; Samson, R., Intra-urban spatial variation of magnetic particles: Monitoring via leaf saturation isothermal remanent magnetisation (SIRM). *Atmospheric Environment* **2012,** *55*, 111-120.

3. Qian, P.; Zheng, X.; Zhou, L.; Jiang, Q.; Zhang, G.; Yang, J., Magnetic properties as indicator of heavy metal contaminations in roadside soil and dust along G312 highways. *Procedia Environmental Sciences* **2011,** *10*, 1370-1375.
4. Chaparro, M. A. E.; Gogorza, C. S. G.; Chaparro, M. A. E.; Irurzun, M. A.; Sinito, A. M., Review of magnetism and heavy metal pollution studies of various environments in Argentina. *Earth Planets Space* **2006,** *58*, 1411-1422.
5. Lu, S.; Yu, X.; Chen, Y., Magnetic properties, microstructure and mineralogical phases of technogenic magnetic particles (TMPs) in urban soils: Their source identification and environmental implications. *Science of the Total Environment* **2016,** *543*, 239-247.
6. Gozzi, F.; Della Ventura, G.; Marcelli, A., Mobile monitoring of particulate matter: State of art and perspectives. *Atmospheric Pollution Research* **2016**, 228-234.
7. CEN CEN/TC 264 - Air quality (EN 12341). https://standards.cen.eu/dyn/www/f?p=204:110:0::::FSP_PROJECT,FSP_ORG_ID:29133,6245&cs=1DC6EB16DD302E384B46A7097AAC67CB5 (14/11/2017),
8. WHO *Health effects of particulate matter. Policy implications for countries in eastern Europe, Caucasus and central Asia.*; 2013.
9. Moreno, E.; Sagnotti, L.; Dinares-Turell, J.; Winkler, A.; Cascella, A., Biomonitoring of traffic air pollution in Rome using magnetic properties of tree leaves. *Atmospheric Environment* **2003**, 2967-2977.
10. Hansard, R.; Maher, B. A.; Kinnersley, R., Biomagnetic monitoring of industry-derived particulate pollution. *Environmental Pollution* **2011,** *159*, 1673-1681.
11. Cao, L.; Appel, E.; Hu, S.; Yin, G.; Lin, H.; Rösler, W., Magnetic response to air pollution recorded by soil and dust-loaded leaves in a changing industrial environment. *Atmospheric Environment* **2015,** *119*, 304-313.
12. Hofman, J.; Lefebvre, W.; Janssen, S.; Nackaerts, R.; Nuyts, S.; Mattheyses, L.; Samson, R., Increasing the spatial resolution of air quality assessments in urban areas: A comparison of biomagnetic monitoring and urban scale modelling. *Atmospheric Environment* **2014,** *92*, 130-140.
13. Hofman, J.; Maher, B. A.; Muxworthy, A. R.; Wuyts, K.; Castanheiro, A.; Samson, R., Biomagnetic monitoring of atmospheric pollution: a review of magnetic signatures from biological sensors. *Environmental Science & Technology* **2017**, 6648-6664.
14. Salo, H.; Bucko, M. S.; Vaahtovuo, E.; Limo, J.; Mäkinen, J.; Pesonen, L. J., Biomonitoring of air pollution in SW Finland by magnetic and chemical measurements of moss bags and lichens. *Journal of Geochemical Exploration* **2012**, 69-81.
15. Vukovic, G.; Urosevic, M. A.; Goryainova, Z.; Pergal, M.; Skrivanj, S.; Samson, R.; Popovic, A., Active moss biomonitoring for extensive screening of urban air pollution: Magnetic and chemical analyses. *Science of the Total Environment* **2015**, 200-210.
16. Kodnik, D.; Winkler, A.; Carniel, F. C.; Tretiach, M., Biomagnetic monitoring and element content of lichen transplants in a mixed land use area of NE Italy. *Science of the Total Environment* **2017,** *595*, 858-867.
17. Wang, G.; Xia, D.; Liu, X.; Chen, F.; Yu, Y.; Yang, L.; Chen, J.; Zhou, A., Spatial and temporal variation in magnetic properties of street dust in Lanzhou City, China. *Chinese Science Bulletin* **2008,** *53*, (12), 1913-1923.
18. Dearing, J. A., *Environmental magnetic susceptibility: Using the Bartington MS2 system*. Chi Publishing: Kenilworth, 1994.
19. Schibler, L.; Boyko, T.; Ferdyn, M.; Gajda, B.; Höll, S.; Jordanova, N.; Rösler, W.; Team, M., Topsoil magnetic susceptibility mapping: data reproducibility and compatibility, measurement strategy. *Studia Geophysica et Geodaetica* **2002**, 43-57.

20. Blundell, A.; Hannam, J. A.; Dearing, J. A.; Boyle, J. F., Detecting atmospheric pollution in surface soils using magnetic measurements: A reappraisal using an England and Wales database. *Environmental Pollution* **2009,** *157*, 2878-2890.
21. Jordanova, N. V.; Jordanova, D. V.; Veneva, L.; Yorova, K.; Petrovsky, E., Magnetic response of soils and vegetation to heavy metal pollution - A case study. *Environmental Science & Technology* **2003**, 4417-4424.
22. Bityukova, L.; Scholger, R.; Birke, M., Magnetic susceptibility as indicator of environmental pollution of soils in Tallinn. *Physics and Chemistry of the Earth* **1999,** *24*, (9), 829-835.
23. Zong, Y.; Xiao, Q.; Lu, S., Magnetic signature and source identification of heavy metal contamination in urban soils of steel industrial city, Northeast China. *Journal of Soils and Sediments* **2017**, 190-203.
24. Magiera, T.; Parzentny, H.; Lukasik, A., The influence of the wind direction and plants on the variability of topsoil magnetic susceptibility in industrial and urban areas of southern Poland. *Environmental Earth Sciences* **2016,** *75*, 213.
25. Magiera, T.; Strzyszcz, Z.; Ferdyn, M.; Gajda, B.; team, M., Screening of anthropogenic dust pollutions in topsoil by using magnetic proxies. In *Environmental Engineering Studies*, Pawlowski, L.; Dudzinska, M.; Pawlowski, A., Eds. Kluwer Academic/Plenum Publishers: New York, 2003; pp 399-407.
26. Fialová, H.; Maier, G.; Petrovsky, E.; Kapicka, A.; Boyko, T.; Scholger, R., Magnetic properties of soils from sites with different geological and environmental settings. *Journal of Applied Geophysics* **2006**, 273-283.
27. Szuszkiewicz, M.; Łukasik, A.; Magiera, T.; Mendakiewicz, M., Combination of geo- pedo- and technogenic magnetic and geochemical signals in soil profiles – Diversification and its interpretation: A new approach. *Environmental Pollution* **2016,** *214*, 464-477.
28. Magiera, T.; Strzyszcz, Z.; Kapicka, A.; Petrovsky, E., Discrimination of lithogenic and anthropogenic influences on topsoil magnetic susceptibility in Central Europe. *Geoderma* **2006,** *130*, (3–4), 299-311.
29. Hanesch, M.; Scholger, R., The influence of soil type on the magnetic susceptibility measured throughout soil profiles. *Geophysical Journal International* **2005,** *161*, 50-56.
30. Karimi, A.; Haghnia, G. H.; Ayoubi, S.; Safari, T., Impacts of geology and land use on magnetic susceptibility and selected heavy metals in surface soils of Mashhad plain, northeastern Iran. *Journal of Applied Geophysics* **2017**, 127-134.
31. Magiera, T.; Jankowski, M.; Switoniak, M.; Rachwal, M., Study of forest soils on an area of magnetic and geochemical anomaly in north-eastern Poland. *Geoderma* **2011,** *160*, 559-568.
32. Hanesch, M.; Rantitsch, G.; Hemetsberger, S.; Scholger, R., Lithological and pedological influences on the magnetic susceptibility of soil: Their consideration in magnetic pollution mapping *Science of the Total Environment* **2007**, 351-363.
33. Blaha, U.; Appel, E.; Stanjek, H., Determination of anthropogenic boundary depth in industrially polluted soil and semi-quantification of heavy metal loads using magnetic susceptibility. *Environmental Pollution* **2008,** *156*, 278-289.
34. Magiera, T.; Parzentny, H.; Róg, L.; Chybiorz, R.; Wawer, M., Spatial variation of soil magnetic susceptibility in relation to different emission sources in southern Poland. *Geoderma* **2015,** *255-256*, 94-103.
35. Spiteri, C.; Kalinski, V.; Rösler, W.; Hoffmann, V.; Appel, E.; team, M., Magnetic screening of a pollution hotspot in the Lausitz area, Eastern Germany: correlation analysis between magnetic proxies and heavy metal contamination in soils. *Environmental Geology* **2005,** *49*, 1-9.
36. Magiera, T.; Zawadzki, J., Using of high-resolution topsoil magnetic screening for assessment of dust deposition: comparison of forest and arable soil datasets. *Environmental Monitoring and Assessment* **2007,** *125*, 19-28.

37. Magiera, T.; Strzyszcz, Z.; Rachwal, M., Mapping particulate pollution loads using soil magnetometry in urban forests in the Upper Silesia industrial region, Poland. *Forest Ecology and Management* **2007,** *248*, 36-42.
38. Magiera, T.; Strzyszcz, Z.; Kapicka, A.; Petrovsky, E., Discrimination of lithogenic and anthropogenic influences on topsoil magnetic susceptibility in Central Europe. *Geoderma* **2006**, 299-311.
39. Heller, F.; Strzyszcz, Z.; Magiera, T., Magnetic record of industrial pollution in forest soils of Upper Silesia, Poland. *Journal of geophysical Research* **1998,** *103*, 767-774.
40. Maier, G.; Scholger, R., Demonstration of connection between pollutant dispersal and atmospheric boundary layers by use of magnetic susceptibility mapping, St. Jacob (Austria). *Physics and Chemistry of the Earth* **2004,** *29*, 997-1009.
41. Kapicka, A.; Jordanova, D.; Petrovsky, E.; Podrazsky, V., Magnetic study of weakly contaminated forest soils. *Water, Air, & Soil Pollution* **2003,** *148*, 31-44.
42. Zawadzki, J.; Fabijanczyk, P.; Magiera, T., The influence of forest stand and organic horizon development on soil surface measurement of magnetic susceptibility. *Polish Journal of Soil Science* **2007,** *40*, 113-124.
43. Magiera, T.; Mendakiewicz, M.; Szuszkiewicz, M.; Jablonska, M.; Chróst, L., Technogenic magnetic particles in soils as evidence of historical mining and smelting activity: A case of the Brynica river valley, Poland. *Science of the Total Environment* **2016**, 536-551.
44. Duan, X.; Hu, S.; Yan, H.; Blaha, U.; Roesler, W.; Appel, E.; Sun, W., Relationship between magnetic parameters and heavy element contents of arable soil around a steel company, Nanjing. **2010**.
45. Evans, M. E.; Heller, F., *Environmental magnetism*. Academic Press: 2003; Vol. 86.
46. Rachwal, M.; Wawer, M.; Magiera, T.; Steinnes, E., Integration of soil magnetometry and geochemistry for assessment of human health risk from metallurgical slag dumps. *Environmental Science and Pollution Research* **2017,** *24*, 26410-26423.
47. Lecoanet, H.; Lévêque, F.; Segura, S., Magnetic susceptibility in environmental applications: comparison of field probes. *Physics of the Earth and Planetary Interiors* **1999**, 191-204.
48. Petrovsky, E.; Hulka, Z.; Kapicka, A., A new tool for in situ measurements of the vertical distribution of magnetic susceptibility in soils as basis for mapping deposited dust. *Environmental Technology* **2004**, 1021-1029.
49. Boyko, T.; Scholger, R.; Stanjek, H.; team, M., Topsoil magnetic susceptibility mapping as a tool for pollution monitoring: repeatability of in situ measurements. *Journal of Applied Geophysics* **2004,** *55*, 249-259.
50. Zawadzki, J.; Fabijanczyk, P.; Magiera, T.; Strzyszcz, Z., Study of litter influence on magnetic susceptibility measurements of urban forest topsoils using the MS2D sensor. *Environmental Earth Sciences* **2010,** *61*, 223-230.
51. Zawadzki, J.; Magiera, T.; Fabijanczyk, P.; Kusza, G., Geostatistical 3-dimensional integration of measurements of soil magnetic susceptibility. *Environmental Monitoring and Assessment* **2012,** *184*, 3267-3278.
52. Fabijanczyk, P.; Zawadzki, J., Improvement of soil magnetic susceptibility measurements performed with MS2D Bartington sensor by removing organic litter subhorizon. *Prace Naukowe Politechniki Warszawskiej. Inżynieria Środowiska* **2010,** *58*, 33-45.
53. Schmidt, A.; Yarnold, R.; Hill, M.; Ashmore, M., Magnetic susceptibility as proxy for heavy metal pollution: a site study. *Journal of Geochemical Exploration* **2005,** *85*, 109-117.
54. D'Emilio, M.; Chianese, D.; Coppola, R.; Macchiato, M.; Ragosta, M., Magnetic susceptibility measurements as proxy method to monitor soil pollution: development of experimental protocols for field surveys. *Environmental Monitoring and Assessment* **2007,** *125*, 137-146.
55. Strzyszcz, Z.; Magiera, T., Magnetic susceptibility and heavy metals contamination in soils of southern Poland. *Physics and Chemistry of the Earth* **1998,** *23*, (9-10), 1127-1131.

56. Freer-Smith, P. H.; Beckett, K. P.; Taylor, G., Deposition velocities to Sorbus aria, Acer campestre, Populus deltoides x trichocarpa 'Beaupré', Pinus nigra and x Cupressocyparis leylandii for coarse, fine and ultra-fine particles in the urban environment. *Environmental Pollution* **2005,** *133*, 157-167.
57. (EEA), E. E. A., Land cover country fact sheets 2012 (Corine Land Cover). In 2012.
58. (ANB), A. N. e. B. Boswijzer 2015. https://www.natuurenbos.be/boswijzer
59. RMI *Klimaatstatistieken van de Belgische gemeenten - Gent (NIS 44021)*.
60. ArcelorMittal *Project-MER: Hervergunning site ArcelorMittal Gent*; 2015.
61. ArcelorMittal *Corporate Responsibility Report*; 2017.
62. Declercq, Y. Luchtpollutie weerspiegeld in magnetische eigenschappen van bodem en vegetatie: een studie in het Gentse havengebied. Faculty of Bioscience Engineering, Department of Soil Management, Ghent University, 2016.
63. VMM, IMJV-databestand. In 2018.
64. VMM, Arcelor Mittal Belgium. In *Pollutant Release and Transfer Register*, 2018-03-13 ed.; 2016.
65. Rachwal, M.; Magiera, T.; Wawer, M., Coke industry and steel metallurgy as the source of soil contamination by technogenic magnetic particles, heavy metals and polycyclic aromatic hydrocarbons. *Chemosphere* **2015**.
66. Dai, Q.; Bi, X.; Wu, J.; Zhang, Y.; Wang, J.; Xu, H.; Yao, L.; Jiao, L.; Feng, Y., Characterization and source identification of heavy metals in ambient PM10 and PM2.5 in an integrated iron and steel industry zone compared with a background site. *Aerosol and Air Quality Research* **2015,** *15*, 875-887.
67. Samson, R.; Wuyts, K.; Koch, K. *AIRbezen Oost-Vlaanderen 2017 Resultaten*; Universiteit Antwerpen - Beweging.net Oost-Vlaanderen: 2017; p 51.
68. VHC Vlaamse havens. https://www.vlaanderen.be/nl/mobiliteit-en-openbare-werken/lucht-en-scheepvaart/vlaamse-havens (2018-05-14),
69. VMM *Luchtkwaliteit in het Vlaamse Gewest. Jaarverslag immissiemeetnetten - 2016*; Vlaamse Milieumaatschappij: Aalst, Belgium, 2017.
70. VMM Resultaten zware metalen in fijn stof en depositie. https://www.vmm.be/data/zware-metalen (2018-05-14),
71. Maher, B. A., Characterisation of soils by mineral magnetic measurements. *Physics of the Earth and Planetary Interiors* **1986,** *42*, 76-92.
72. Thompson, R.; Oldfield, F., Soil magnetism. In *Environmental Magnetism*, Springer: Dordrecht, 1986; pp 72-87.
73. Derese, C.; Vandenberghe, D. A. G.; Zwertvaegher, A.; Court-Picon, M.; Crombé, P.; Verniers, J.; Van den haute, P., The timing of aeolian events near archaeological settlements around Heidebos (Moervaart area, N Belgium). *Netherlands Journal of Geosciences - Geologie en mijnbouw* **2010,** *89*, (3), 173-186.
74. Jordanova, N., *Soil magnetism: applications in pedology, environmental science and agriculture*. Academic press: Amsterdam, 2017.
75. De Moor, G.; Heyse, I., Lithostratigrafie van de Kwartaire afzettingen in de overgangszone tussen de kustvlakte en de Vlaamse Vallei in Noordwest België. *Natuurwetenschappelijk Tijdschrift* **1974,** *56*, 85-109.
76. DOV-Vlaanderen WRB Soil Units (1:40.000). https://www.dov.vlaanderen.be/kaarten (17/01/2018),
77. ESHER *Uitgebreid bosbeheersplan voor het Kloosterbos*; Ghent, 2006.
78. Burov, B. V.; Nourgaliev, D. K.; Jasonov, P. G., *Paleomagnetic analysis*. Kazan University Press: Kazan, 1986.
79. Jasonov, P. G.; Nourgaliev, D. K.; Burov, B. V.; Heller, F., A modernized coercivity spectrometer. *Geologica Carphatica* **1998,** *49*, 224-225.
80. Hooda, P. S., *Trace elements in soils*. Blackwell Publishing Ltd: 2010.

81. Van Ranst, E.; Verloo, M.; Demeyer, A.; Pauwels, M., *Manual for the soil chemistry and fertility laboratory - analytical methods for soils and plants, equipment, and management of consumables*. Ghent University: GHent, Belgium, 1999.
82. Tomlinson, D. L.; Wilson, J. G.; Harris, C. R.; Jeffrey, D. W., Problems in the assessment of heavy-metal levels in estuaries and the formation of a pollution index. *Helgoländer Meeresuntersuchungen* **1980**, 566-575.
83. Logsdon, S.; Clay, D.; Moore, D.; Tsegaye, T., *Soil science: Step-by-step field analysis*. Soil Science Society of America: Madison, USA, 2008.
84. ISO 11277:2009 - Soil quality - Determination of particle size distribution in mineral soil material - Method by sieving and sedimentation. In.
85. Walkley, A.; Black, I. A., An examination of the Degtjareff method for determining soil organic matter, and a proposed modification of the chromic titration method. *Soil Science* **1934,** *37*, 29-38.
86. (ISO), I. O. f. S., ISO 10390:2005 - Soil quality - Determination of pH. In 2015.
87. Nelson, R. E., Carbonate and gypsum. In *Methods of Soil Analysis, Part 2. Chemical and Microbiological Properties*, American Society of Agronomy: Madison, Wisconsin, 1982; pp 181-197.
88. Webster, R.; Lark, R. M., *Field sampling for environmental science and management*. Routledge: USA, Canada, 2013; p 192.
89. Tukey, J. W., *Exploratory data analysis*. Addison-Wesley Publishing Company: 1977.
90. Dearing, J. A.; Dann, R. J. L.; Hay, K.; Lees, J. A.; Loveland, P. J.; Maher, B. A.; O'Grady, K., Frequency-dependent susceptibility measurements of environmental materials. *Geophysical Journal International* **1996,** *124*, 228-240.
91. Gautam, P.; Blaha, U.; Appel, E., Integration of magnetism and heavy metal chemistry of soils to quantify the environmental pollution in Kathmandu, Nepal. *The Island Arc* **2005**, 424-435.
92. King, J.; Banerjee, S. K.; Marvin, J.; Özdemir, Ö., A comparison of different magnetic methods of determining the relative grain size of magnetite in natural materials: some results from lake sediments. *Earth and Planetary Science Letters* **1982,** *59*, 404-419.
93. Boyle, J. F.; Dearing, J. A.; Blundell, A.; Hannam, J. A., Testing competing hypotheses for soil magnetic susceptibility using a new chemical kinetic model. *Geology* **2010,** *38*, (12), 1059-1062.
94. GeopuntVlaanderen Geopunt-kaart. https://www.geopunt.be/
95. Nicholson, F. A.; Smith, S. R.; Alloway, B. J.; Carlton-Smith, C.; Chambers, B. J., An inventory of heavy metals inputs to agricultural soils in England and Wales. *Science of the Total Environment* **2003,** *311*, 205-219.
96. Bradl, H. B., Sources and origins of heavy metals. In *Heavy Metals in the Environment*, Elsevier Ltd.: London, UK, 2005; Vol. 6.

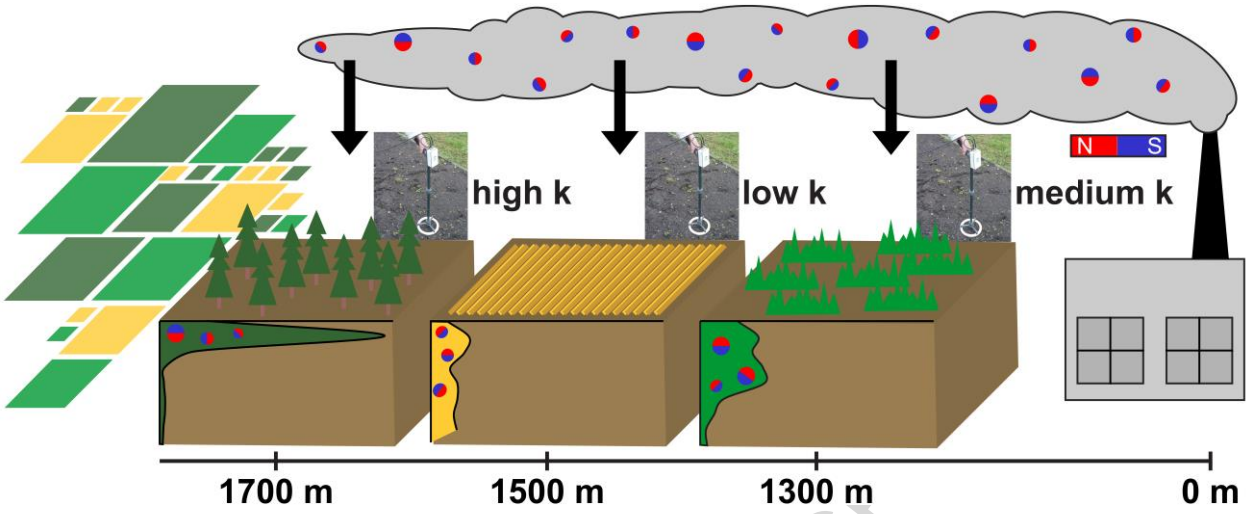


Graphical abstract

**Highlights**

- 3D magnetic soil variation was studied across different land use classes
- land use affected magnetic susceptibility, limiting direct evaluation of pollution
- magnetic susceptibility did not correlate with the distance to the pollution source
- downhole measurements facilitated correct interpretation of topsoil magnetic maps
- robust magnetic monitoring across various land use classes requires ancillary data